

## RESEARCH ARTICLE

# Preparation of the alpha-emitting prostate-specific membrane antigen targeted radioligand [ $^{212}\text{Pb}$ ]Pb-NG001 for prostate cancer

Vilde Yuli Stenberg<sup>1,2,3</sup>  | Asta Juzeniene<sup>1</sup>  | Qingqi Chen<sup>4</sup>  |  
Xiaoming Yang<sup>4</sup>  | Øyvind Sverre Bruland<sup>3,5</sup>  | Roy Hartvig Larsen<sup>2</sup>

<sup>1</sup>Department of Radiation Biology, Institute for Cancer Research, Norwegian Radium Hospital, Oslo University Hospital, Oslo, Norway

<sup>2</sup>Department of Research and Development, Nucligen AS, Oslo, Norway

<sup>3</sup>Institute for Clinical Medicine, University of Oslo, Oslo, Norway

<sup>4</sup>Department of Drug Synthesis, MedKoo Biosciences, Morrisville, North Carolina

<sup>5</sup>Department of Oncology, Norwegian Radium Hospital, Oslo University Hospital, Oslo, Norway

## Correspondence

Asta Juzeniene, Department of Radiation Biology, Institute for Cancer Research, Norwegian Radium Hospital, Oslo University Hospital, Montebello, 0379 Oslo, Norway.  
Email: asta.juzeniene@rr-research.no

## Funding information

Norwegian Research Council, Grant/Award Number: 290639; Nucligen AS; Sciencons AS

Prostate-specific membrane antigen (PSMA) is the most promising target for radioligand therapy of prostate cancer. The aim of this study was to prepare a small molecular ligand p-SCN-Bn-TCMC-PSMA (NG001) and compare it with the commonly used DOTA-based PSMA-617. The PSMA-targeting ability of the  $^{212}\text{Pb}$ -labelled ligands was evaluated using PSMA-positive C4-2 human prostate cancer cells. Lead-212 is an in vivo generator of alpha particles by its daughter nuclides  $^{212}\text{Bi}$  and  $^{212}\text{Po}$ . NG001 was synthesized by conjugating the isothiocyanato group of p-SCN-Bn-TCMC to the amino group of a glutamate-urea-based PSMA-binding entity. Molecular size, chelator unit and chelator linking method are different in NG001 and PSMA-617. Both ligands were efficiently labelled with  $^{212}\text{Pb}$  using a  $^{224}\text{Ra}/^{212}\text{Pb}$ -solution generator in transient equilibrium with progeny. Lead-212-labelled NG001 was purified with a yield of  $85.9\pm 4.7\%$  and with  $0.7\pm 0.2\%$  of  $^{224}\text{Ra}$ . Compared with [ $^{212}\text{Pb}$ ]Pb-PSMA-617, [ $^{212}\text{Pb}$ ]Pb-NG001 displayed a similar binding and internalization in C4-2 cells, with comparable tumour uptake in mice bearing C4-2 tumours, but almost a 2.5-fold lower kidney uptake. Due to the rapid normal tissue clearance and tumour cell internalization, any significant translocalization of  $^{212}\text{Bi}$  was not detected in mice. In conclusion, the obtained results warrant further preclinical studies to evaluate the therapeutic efficacy of [ $^{212}\text{Pb}$ ]Pb-NG001.

## KEYWORDS

$^{212}\text{Pb}$ , DOTA, prostate cancer, p-SCN-Bn-TCMC-PSMA-ligand, PSMA-617

## 1 | INTRODUCTION

The prostate-specific membrane antigen (PSMA) is highly expressed in metastatic castrate-resistant prostate cancer (mCRPC) with limited expression in healthy tissues and correlates with a dismal prognosis.<sup>1,2</sup> The

majority of bone, visceral, and lymph-node metastases highly express PSMA,<sup>1,2</sup> making PSMA an ideal target for radioligand therapy (RLT) of mCRPC.<sup>3,4</sup> A variety of low molecular weight PSMA-targeting ligands have been synthesized, labelled with radionuclides, and tested in both preclinical and clinical trials.<sup>3-5</sup> In

This is an open access article under the terms of the Creative Commons Attribution-NonCommercial-NoDerivs License, which permits use and distribution in any medium, provided the original work is properly cited, the use is non-commercial and no modifications or adaptations are made.

© 2020 The Authors. Journal of Labelled Compounds and Radiopharmaceuticals published by John Wiley & Sons Ltd

general, PSMA-targeting ligands have a PSMA-binding region (motif), a linker (spacer), and a chelator (moiety for radiolabelling).<sup>5</sup> The linker region is used to adjust molecular size and polarity to impact the in vivo distribution properties.<sup>5-7</sup> The most studied PSMA ligands for therapeutic use, PSMA-617 and PSMA-I&T, have different linkers, while the binding motif (glutamate-urea moiety) and the chelating moiety (1,4,7,10-tetraazacyclododecane-1,4,7,10-tetraacetic acid [DOTA]) are the same. PSMA-617 and PSMA-I&T labelled with the beta emitter <sup>177</sup>Lu ( $t_{1/2} \approx 6.7$  days) and MIP-1095 labelled with the beta emitter <sup>131</sup>I ( $t_{1/2} \approx 8.0$  days) have been investigated in preclinical and clinical studies.<sup>7-11</sup> A recent meta-analysis of 17 studies demonstrated that RLT with [<sup>177</sup>Lu]Lu-PSMA-617 and [<sup>177</sup>Lu]Lu-PSMA-I&T is an effective treatment for mCRPC with low toxicity.<sup>10</sup> However, around 30% of patients do not respond to [<sup>177</sup>Lu]Lu-PSMA RLT.<sup>12</sup> It has already been demonstrated that RLT with PSMA-617 labelled with the alpha emitter <sup>225</sup>Ac ( $t_{1/2} \approx 9.9$  days) may overcome this radioresistance.<sup>12</sup> Recent clinical studies have reported that targeted alpha therapy (TAT) using <sup>225</sup>Ac- and <sup>213</sup>Bi-labelled PSMA ligands is a promising treatment of mCRPC.<sup>3,12-14</sup> Despite the great efficacy, their limited supply,<sup>15</sup> the toxicity in salivary glands of <sup>225</sup>Ac,<sup>13</sup> and the short half-life of <sup>213</sup>Bi ( $t_{1/2} \approx 46$  minutes)<sup>15</sup> warrant to explore other alpha-emitting radionuclides for PSMA-RLT.

The use of alpha emitters for cancer therapy has several advantages over beta emitters. The short range of alpha radiation in tissue (<0.1 mm), corresponding to only a few cell diameters, allows the selective killing of cancer cells and reduction of side effects in surrounding healthy cells.<sup>16</sup> At the same time, the high energy of alpha particles (several MeV) and their high linear energy transfer (>100 keV/ $\mu$ m) lead to effective cell killing via DNA double-strand breaks, which are largely independent of cell cycle and oxygenation status.<sup>16</sup>

Lead-212 is a beta emitter that generates alpha particle radiation via its short-lived progenies <sup>212</sup>Bi ( $t_{1/2} \approx 60.6$  minutes) and <sup>212</sup>Po ( $t_{1/2} \approx 0.3$  microseconds). DOTA-conjugated monoclonal antibodies (mAb) form stable complexes with <sup>212</sup>Pb.<sup>17-19</sup> However, one third of <sup>212</sup>Bi could be lost from the DOTA complex during <sup>212</sup>Pb decay.<sup>20,21</sup> Furthermore, acid-catalysed dissociation of <sup>212</sup>Pb from DOTA conjugates after internalization has been reported as a source of bone marrow toxicity, as released <sup>212</sup>Pb is transported to the bone where it subsequently decays to <sup>212</sup>Bi.<sup>17,22,23</sup> Replacement of the carboxylic acid donor arms of DOTA with amide arms has yielded the chelator S-2-(4-Isothiocyanatobenzyl)-1,4,7,10-tetraaza-1,4,7,10-tetra(2-carbamoylmethyl)cyclododecane (TCMC), which to date is the best available chelator for

<sup>212</sup>Pb.<sup>17-19</sup> The complex of lead cation and TCMC is less labile to metal ion release under lower pH conditions, conferring enhanced resistance to acid-catalysed dissociation within the cell.<sup>17-19</sup> A recent clinical trial has demonstrated that no acute or late toxicity occurred in patients with ovarian cancer treated with [<sup>212</sup>Pb]Pb-TCMC-trastuzumab.<sup>24</sup> TAT with [<sup>212</sup>Pb]Pb-octreotate has also shown a favourable safety profile in patients with neuroendocrine tumours.<sup>25</sup>

The kidneys are a possible dose-limiting organ because of the predominant renal excretion of PSMA ligands.<sup>26</sup> The high uptake of <sup>177</sup>Lu- and <sup>225</sup>Ac-labelled PSMA ligands in kidneys is usually observed short time (1-4 hours) after injection of the radioligands, in both mice and humans.<sup>27,28</sup> With shorter-lived radionuclides like <sup>212</sup>Pb ( $t_{1/2} \approx 10.6$  hours) and <sup>211</sup>At ( $t_{1/2} \approx 7.2$  hours), the initial kidney uptake could represent a potential toxicity problem since a high dose will be delivered to the kidneys within the first few hours.<sup>29,30</sup> It would therefore be advantageous to have a novel PSMA ligand with less kidney uptake without compromising the high tumour targeting documented with PSMA-617 and PSMA-I&T. Recently, two groups have developed several novel PSMA-seeking ligands (CA008, CA009/NG001, CA011, CA012, L1, L2, L3, L4 and L5) and studied their use for targeting with lead.<sup>30,31</sup> Since measurement of localization of <sup>212</sup>Pb and daughters in vivo is complicated,<sup>21</sup> <sup>203</sup>Pb was used as a surrogate for <sup>212</sup>Pb in their biodistribution studies.<sup>30,31</sup> Lead-203 ( $t_{1/2} \approx 52$  hours) decays by electron capture followed by emission of gamma photons of 279 keV (81%), 401 keV (5%), and 680 keV (0.9%). It decays to stable <sup>203</sup>Tl. The energy of gamma photons and the absence of daughters in the decay of <sup>203</sup>Pb make <sup>203</sup>Pb particularly suitable for the biodistribution studies of lead complexes. However, dosimetric estimates from <sup>203</sup>Pb data may not necessarily give the complete picture of alpha particle exposure using <sup>212</sup>Pb conjugates since there is a possibility that <sup>212</sup>Bi can be released from <sup>212</sup>Pb complexes during <sup>212</sup>Pb decay<sup>32</sup> and in the case of DOTA at low intracellular pH.<sup>20,23</sup> Early studies on the metabolism of [<sup>212</sup>Pb]Pb-DOTA-mAb and [<sup>212</sup>Pb]Pb-DOTMP in mice demonstrated the translocation of <sup>212</sup>Bi from the target site and its preferential accumulation in kidneys,<sup>23,33</sup> which may lead to toxicity. The distribution of <sup>212</sup>Bi in different organs after administration of [<sup>212</sup>Pb]Pb-PSMA ligands is currently unknown.

The aim of this study was to compare in vitro and in vivo characteristics of <sup>212</sup>Pb-labelled p-SCN-Bn-TCMC-PSMA ligand (NG001) and PSMA-617. The PSMA-targeting properties of [<sup>212</sup>Pb]Pb-NG001 and [<sup>212</sup>Pb]Pb-PSMA-617 were evaluated using PSMA-positive C4-2 prostate cancer cells. Biodistributions of <sup>212</sup>Pb and <sup>212</sup>Bi

were studied in different organs. The ligand NG001 was invented and patented by Larsen.<sup>34</sup> A <sup>203</sup>Pb-labelled CA009 (identical to the structure of NG001) was presented by Dos Santos et al.<sup>31</sup> The current study is the first presentation in the scientific literature regarding <sup>212</sup>Pb-labelled NG001.

## 2 | EXPERIMENTAL

### 2.1 | Synthesis of NG001 and PSMA-617

The chelator p-SCN-Bn-TCMC and the ligand PSMA-617 were synthesized following procedures reported in the

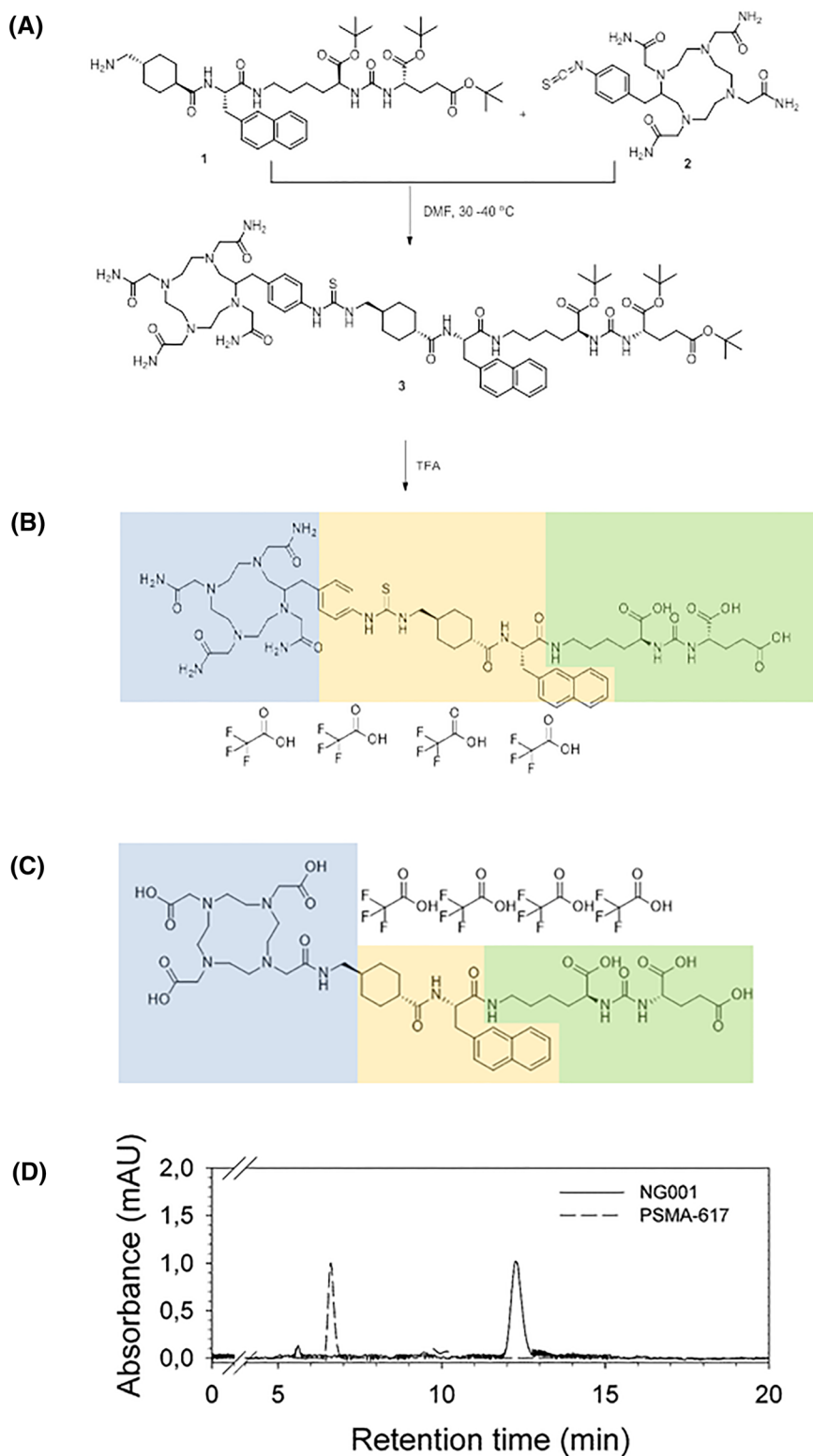


**FIGURE 1** Synthetic route of NG001. DMF, dimethylformamide; TFA, trifluoroacetic acid(A). Compounds are named **1**, **2** and **3**. Chemical structures of (B) NG001 and (C) PSMA-617. Chelating entity for labelling (blue), linker region (yellow) and binding motif (green). Representative chromatograms of NG001 and PSMA-617(D). The UV absorption was measured at 220 nm (mAU, milli absorbance unit)

literature.<sup>17,35</sup> The synthesis of NG001 is summarized in Figure 1.

Synthesis of compound **3**. di-tert-butyl (((2S)-1-(tert-butoxy)-6-((2S)-3-(naphthalen-2-yl)-2-((1R,4S)-4-((3-(4-((1,4,7,10-tetrakis(2-amino-2-oxoethyl)-1,4,7,10-tetraazacyclododecan-2-yl)methyl)phenyl)thioureido)methyl)cyclohexane-1-carboxamido)propanamido)-1-oxohexan-2-yl)carbonyl)-L-glutamate. Eighty-two milligrams of compound **1** was stirred with 60 mg of compound **2** in 5 mL dimethylformamide at 30 to 40°C until completion. The solvent was removed in vacuo, and the residue was subject to the separation on Sephadex LH20 using methanol as the eluent. The fractions containing compound **3** were pooled and concentrated in vacuo at a bath temperature of 30°C. The synthesis of compound **3** resulted in a light yellow glassy solid (96 mg) at a yield of 70% and purity of 98% as determined by high-performance liquid chromatography (HPLC).

Synthesis of NG001 (((1S)-1-carboxy-5-((2S)-3-(naphthalen-2-yl)-2-((1R,4S)-4-((3-(4-((1,4,7,10-tetrakis(2-amino-2-oxoethyl)-1,4,7,10-tetraazacyclododecan-2-yl)methyl)phenyl)thioureido)methyl)cyclohexane-1-carboxamido)propanamido)pentyl)carbonyl)-L-glutamic acid tetrakis (trifluoroacetic acid): Ninety milligrams of compound **3** was stirred in 0.5 mL of anisole and 3 mL of trifluoroacetic acid (TFA) at room temperature for 1 hour. The solvent was removed in vacuo to give a light yellow oil. The oil was triturated in 10 mL of ethyl acetate for 30 minutes, and the off-white solids were filtered off; washed sequentially with ethyl acetate, acetone and ether; and dried in vacuo overnight to give 94 mg of NG001 as the TFA salt. A product with a yield of 86% and purity of 98% (HPLC) was obtained. Liquid chromatography/mass spectrometry (LC/MS) ( $C_{57}H_{82}N_{14}O_{13}S$ );  $m/z$  (electrospray ionization [ESI] positive) = 1203;  $m/z$  (ESI negative) = 1202. <sup>1</sup>H-NMR (DMSO-d<sub>6</sub>, ppm): 7.69-7.95 (m, 10H), 7.39-7.49 (m, 7H), 7.21 (m, 2H), 6.27-6.33 (m, 2H), 4.53 (m, 2H), 4.11 (m, 1H), 4.02 (m, 1H), 3.35-3.93 (m, 24H), 3.03-3.20 (m, 6H), 2.80-2.99 (m, 6H), 2.24 (m, 2H), 2.10 (m, 1H), 1.87-1.98 (m, 1H), 1.45-1.73 (m, 8H), 1.19-1.32 (m, 5H), 1.05-1.11 (m, 1H), 0.86-0.91 (m, 1H).

Proton spectra were recorded on a Varian 400 MHz NMR. LC/MS data were obtained using a quadrupole mass spectrometer on Shimadzu LC/MS 2010 (column Sepax ODS 50 mm × 2.0 mm, 5 μm) or Agilent 1200 HPLC, 1956 MSD (column Shim-pack XR-ODS 30 mm × 3.0 mm, 2.2 μm) operating in ES (+) ionization mode. All final compounds were greater than 95% pure based on HPLC UV% AUC. Structures were determined by <sup>1</sup>H NMR and LC/MS. Analytical thin-layer chromatography (TLC) was carried out using EMD silica gel 60 F254 TLC plates. TLC visualization was achieved with a UV lamp or in an iodine chamber. Flash column

chromatography was done on a CombiFlash Companion system using Isco prepacked silica gel columns. Unless otherwise stated, reagent grade chemicals were obtained from commercial sources and were used without further purification.

The ligands were purified by HPLC to a purity of >98%, dried, and stored as the TFA salt.

## 2.2 | Calculation of molecular properties

Predicted molecular properties of compounds were calculated using the free molecular calculation services provided by Molinspiration Cheminformatics (<https://www.molinspiration.com/>).<sup>36</sup>

LogP (octanol/water partition coefficient) is calculated by the methodology developed by Molinspiration as a sum of fragment-based contributions and correction factors.

Topological polar surface area (TPSA) is calculated based on the methodology published by Ertl et al<sup>37</sup> as a sum of fragment contributions; O- and N-centred polar fragments are considered.

Method for calculation of molecule volume developed at Molinspiration is based on group contributions. These have been obtained by fitting sum of fragment contributions to “real” 3D volume for a training set of about 12 000, mostly drug-like molecules. Three-dimensional molecular geometries for a training set were fully optimized by the semiempirical AM1 method. Calculated volume is expressed in cubic Angstroms (Å<sup>3</sup>).

## 2.3 | Reverse phase HPLC

Twenty microlitres of sample solution were injected by an autosampling injector (Gilson 234, Gilson, France) into a reverse phase Hichrom H5ODS-10606 column of dimensions 250 × 4.6 mm (Hichrom Ltd., Theale, Reading Berkshire, UK). The mobile phase of the isocratic method consisted of HPLC-grade acetonitrile, water and TFA (25:74:1 v/v) purchased from Fisher Chemicals (Västra Frölunda, Sweden). A low-pressure gradient pump system (P680A LPG, Dionex, Germering, Germany) with integrated degasser was used to generate a flow rate of 1.5 mL/minutes. The column effluent was monitored at 280 nm by a Spectra 200 UV detector (Newport Spectra-Physics, Darmstadt, Germany) connected to the chromatography interface UCI-100 (Dionex). All the chromatographic separations were carried out at ambient temperature. Chromeleon software (version 6.50, Dionex) was used for data acquisition and for calculation of the peak areas.

## 2.4 | Preparation of radionuclides and radioactivity measurements

Radium-224 was extracted from a generator column containing actinide resin (Eichrom Technologies, Lisle, Illinois) with immobilized  $^{228}\text{Th}$  (Eckert & Ziegler, Braunschweig, Germany) by eluting with 1 M HCl.<sup>32,38</sup> The  $^{224}\text{Ra}$  was free of  $^{228}\text{Ra}$ ,  $^{226}\text{Ra}$  and  $^{223}\text{Ra}$  as demonstrated by decay analyses, and thereby, is carrier-free. The details of the  $^{224}\text{Ra}/^{212}\text{Pb}$ -solution generator setup have been described elsewhere.<sup>32,38</sup> Radioactive samples were measured on a Cobra II Autogamma counter (Packard Instrument Company, Downer Grove, Illinois) and Hidex Automatic Gamma counter (Hidex Oy, Turku, Finland) with the counting window setting from 60 to 110 keV. This setting mainly gives the  $^{212}\text{Pb}$  activity (34.9% relative to the mother nuclide  $^{224}\text{Ra}$ ) with very little contribution (1.2% relative to  $^{224}\text{Ra}$ ) from other radionuclides in the  $^{224}\text{Ra}$  series (Table S1).

Radium-224 activity was indirectly determined by measuring  $^{212}\text{Pb}$  activity after 4 to 5 days when the initial  $^{212}\text{Pb}$  had decayed and equilibrium between  $^{224}\text{Ra}$  and newly formed  $^{212}\text{Pb}$  had been reached. A Capintec CRC-25R radioisotope dose calibrator (Capintec Inc., Ramsey, New Jersey) and a liquid nitrogen cooled high-purity Germanium (HPGe) radiation detector (Canberra Industries Inc, Meriden, Connecticut) combined with the Genie 2000 Spectroscopy Software (Canberra) were used during the radiolabelling procedures.

## 2.5 | Radiolabelling of NG001 and PSMA-617

The PSMA ligands were dissolved in 0.5 M ammonium acetate ( $\text{NH}_4\text{OAc}$ ) in 0.1 M HCl at a concentration of 1 mg/mL. NG001 or PSMA-617 (1–7  $\mu\text{g}$ ) was added to the  $^{224}\text{Ra}$ -solution (2–5 MBq/mL) in equilibrium with progeny in 0.5 M  $\text{NH}_4\text{OAc}$  in 0.1 M HCl, adjusted to pH 5 to 6. The reaction mixture was incubated for 30 minutes on a Thermomixer (Eppendorf, Hamburg, Germany) at 37°C and 450 rpm. Different concentrations of ligand were radiolabelled, typically in the range of 20 to 80  $\mu\text{g}/\text{mL}$ . The labelling reactions were evaluated by radiochemical purity (RCP) determination by TLC using instant TLC strips (Tec-control, Biodex, New York).

## 2.6 | Purification of $^{212}\text{Pb}$ -labelled PSMA ligands from $^{224}\text{Ra}/^{212}\text{Pb}$ -solution generator

Lead-212-labelled NG001 and PSMA-617 were purified using PD Minitrap G-10 columns prepacked with

Sephadex G-10 resin (exclusion limit,  $M_r$  cut-off of 0.7 kDa, GE Healthcare Bio-Sciences AB, Uppsala, Sweden) to remove  $^{224}\text{Ra}$  and other unconjugated daughter nuclides. The column was equilibrated with 8 to 9 mL of 0.9% NaCl before the reaction mixture was loaded onto the top of the column. After the sample had entered the packed bed, 0.9% NaCl was added to a total volume of 0.25 to 0.30 mL. During the elution process, 10 fractions of around 0.25 mL were collected in Eppendorf tubes and activity of each fraction was measured with a germanium detector. Typically, the radiolabelled ligand was eluted in fractions 3 to 7. The yield of radiolabelled ligand in each fraction was calculated by Equation (1).

$$\text{Yield of radioligand in Fraction (\%)} = \frac{\text{Activity in fraction (kBq)}}{\text{Total activity (kBq)} \times \text{RCP}} \times 100. \quad (1)$$

Total activity loaded onto the column was determined by measuring the sample in the HPGe detector immediately before purification. After 4 to 5 days, the  $^{212}\text{Pb}$  activity of the purified product was measured to determine the amount of  $^{224}\text{Ra}$  present in the sample.

## 2.7 | Cell culture

The PSMA-expressing prostate cancer cell line C4-2 (ATCC CRL3314, Manassas, Virginia)<sup>38</sup> was grown as monolayer in RPMI 1640 medium (Sigma-Aldrich Norway AS, Oslo, Norway) supplemented with 10% heat inactivated fetal bovine serum (FBS, GE Healthcare Life Sciences, Chicago, Illinois), 100 units/mL penicillin and 100  $\mu\text{g}/\text{mL}$  streptomycin (Sigma-Aldrich) at 37°C in a humid atmosphere with 95% air and 5%  $\text{CO}_2$ .

## 2.8 | Radiolytic stability of [ $^{212}\text{Pb}$ ]Pb-NG001

Stability of purified [ $^{212}\text{Pb}$ ]Pb-NG001 stored 1:1 in phosphate-buffered saline (PBS) or FBS was tested by TLC analysis after different time points up to 48 hours.

## 2.9 | Binding and internalization of $^{212}\text{Pb}$ -labelled NG001 and PSMA-617 in C4-2 cells

Saturation radioligand binding was measured in C4-2 cells by incubating  $10^6$  cells in 0.2 mL of PBS with 0.5% bovine serum albumin (BSA, Sigma-Aldrich) with eight

different radioligand concentrations (3–200 nM) for 1 hour at 37°C and 450 rpm. Nonspecific binding was estimated by blocking cells with an excess of unlabelled ligand, 12 000 nM, 15 minutes before addition of radioligand. Activities of the samples were measured in a gamma counter before (added activity) and after cells had been washed 3 times with PBS with 0.5% BSA (cell bound activity). The number of specifically bound ligands per cell was plotted against ligand concentration and equilibrium dissociation constants ( $k_d$ ) for the radioligands were determined by nonlinear regression (Sigmaplot version 14.0, Systat Software, Inc., San Jose, California).

Before radioligand injection in the biodistribution studies, binding of the radiolabelled ligands was verified by a similar cell binding assay. In this assay, 10 to 12 × 10<sup>6</sup> cells were incubated with 1.5 to 6 nM of radioligand. The cell binding fraction (% cell bound activity of added activity) was estimated by subtracting nonspecific cell bound activity from total cell bound activity.

For the internalization study, C4-2 cells (10<sup>5</sup> cells/well) were seeded 1 day prior to the experiment into poly-L-lysine (Sigma-Aldrich, Oslo, Norway) coated 24-well plates (1 mL/well, Thermo Fisher Scientific, Roskilde, Denmark) and treated as described by Dos Santos et al.<sup>31</sup>

The culture medium was removed, and the cells were washed once with 0.5 mL Opti-MEM reduced serum medium (Gibco from Thermo Fisher Scientific). After that, 0.22 mL/well Opti-Mem medium alone or with 500 μM PSMA inhibitor 2-(phosphonomethyl)pentane-1,5-dioic acid (2-PMPA, Sigma-Aldrich) solution was added for 15 minutes at 37°C. Following the addition of 30 μL of [<sup>212</sup>Pb]Pb-NG001 or [<sup>212</sup>Pb]Pb-PSMA-617, the cells were then incubated for 45 minutes at 37°C on an orbital shaker. Incubation was terminated by removal of the incubation medium. The cells were washed 3 times with 1 mL ice cold PBS. A half mL of 50 mM glycine buffer (pH 2.8) was added to each well chosen for internalization experiment and incubated for 5 minutes at room temperature to remove surface-bound radioactivity. The supernatant was collected, and cells were washed with ice-cold PBS (1 mL/well). A half mL of 0.3 M NaOH was added to wells for 10 minutes at room temperature to lyse the cells. The cell-associated radioactivity of the collected lysed cells was measured using a gamma counter for 1 minute. The standards were also measured at the same time. The additional wells with the cells were trypsinized and counted. The final results were calculated as %IA/10<sup>6</sup> cells (%IA = percentage of added radioactivity). All experiments were performed in triplicate.

## 2.10 | Animals

Eighteen Hsd: Athymic Nude-Foxn1<sup>nu</sup> mice bred at the Comparative Medicine at the Norwegian Radium Hospital (Oslo University Hospital, Oslo, Norway) were used in this study. Cages (up to five mice per cage) were housed in a Scantainer (Scanbur, Nittedal, Norway) under pathogen-free conditions with a 12-hour light cycle at a constant temperature (24°C) and humidity (60%). Animals had ad libitum access to food and water, and environmental enrichment was provided. The mice were around 10 to 12 weeks in age, weighing between 25 and 35 g, at the start of the study. All procedures and experiments involving animals in this study were approved by the National Animal Research Authority (Oslo, Norway) and carried out in accordance with the European Convention for the Protection of Vertebrates Used for Scientific Purposes [Scientific Procedures] Act 1986, as well as the ARRIVE guidelines.

Mice were inoculated subcutaneously in both flanks with 10<sup>7</sup> C4-2 cells in RPMI1640 medium (without supplements) mixed 1:1 with Matrigel Matrix (Corning, New York), in a total volume of 200 μL. Prior to cell inoculation, the absence of murine contaminations in the human cell line was verified by a polymerase chain reaction-based pathogen test (IMPACT I, IDEXX Bioanalytics, Ludwigsburg, Germany). The tumours were allowed to grow to reach a volume of 250 to 1000 mm<sup>3</sup>, and tumour-bearing mice were randomized based on tumour size before radioligand injection.

Mice were monitored 2 times per week for changes in weight and tumour size and for any sign of illness or discomfort. Humane end points were >15% weight loss from initial weight, tumours that exceed 15 mm in any direction, ulcerate or interfere with normal behaviour, or any signs of severe sickness or discomfort. No mice became ill or died prior to the experimental end point.

## 2.11 | Biodistribution of <sup>212</sup>Pb and its daughter <sup>212</sup>Bi in different organs following administration of [<sup>212</sup>Pb]Pb-NG001 and [<sup>212</sup>Pb]Pb-PSMA-617 in athymic mice with C4-2 xenografts

The radiolabelled ligands were purified by desalting gel exclusion, as described above, and sterile-filtered immediately before injections. Hsd: Athymic Nude-Foxn1<sup>nu</sup> mice bearing C4-2 tumours were injected intravenously via tail vein with 10 to 56 kBq (0.06–0.60 nmol) of [<sup>212</sup>Pb]Pb-NG001 (n=11) or 79 kBq (0.49 nmol) of [<sup>212</sup>Pb]Pb-PSMA-617 (n=4) in a volume of 100 μL. Two or 24 hours after

injection, the mice were given gas anaesthesia (~3.5% Sevofluran (Baxter, IL) in oxygen at a flow rate of 0.5 L/minutes) for blood collection by cardiac puncture. Mice were then euthanized by cervical dislocation, urine collected and different organs/tissues harvested. Weight and activity of each tissue sample were measured in a gamma counter, and the decay corrected % injected dose per gram tissue (%ID/g) was calculated. Samples of the injectates were used as references in the measurement procedures.

Measurements were performed in two windows, 60 to 110 keV (mainly  $^{212}\text{Pb}$  activity) and 520 to 640 (mainly  $^{208}\text{Tl}$  activity), within 1 hour after sacrifice (Day 0), the next day (Day 1) and 5 days (Day 5) after injection of [ $^{212}\text{Pb}$ ]Pb-PSMA ligands. At Day 0, when 0.5 hour have passed,  $^{208}\text{Tl}$  is in equilibrium with its mother,  $^{212}\text{Bi}$ , and can be used to determine  $^{212}\text{Bi}$  activity in the tissue sample since  $^{208}\text{Tl}$  present at time 0 has decayed and everything present at 0.5 hour comes from decay of  $^{212}\text{Bi}$  in the sample. Lead-212 measurements at Day 0 may contain a contribution from nonequilibrium excess  $^{212}\text{Bi}$ , while the measurements at Day 1 reflect the amount of solely  $^{212}\text{Pb}$  present as all of its progenies present at time 0 has decayed. Therefore,  $^{212}\text{Pb}$  activity measured at Day 1 was decay-corrected to Day 0 to calculate the correct %ID/g values. After 5 days,  $^{224}\text{Ra}$  activity was determined from  $^{212}\text{Pb}$  activity as initial  $^{212}\text{Pb}$  had decayed and equilibrium between  $^{224}\text{Ra}$  and newly formed  $^{212}\text{Pb}$  had been reached. After purification of the radioligands, only a negligible amount (<1%) of  $^{224}\text{Ra}$  was present in the injectate. The ingrowth of  $^{212}\text{Pb}$  from  $^{224}\text{Ra}$  was calculated and used to correct the  $^{212}\text{Pb}$  values.

## 2.12 | Statistics

The data sets were analysed for significance using the one-way analysis of variance using SigmaPlot 14.0 software. A *P*-value of <.05 was considered statistically significant.

## 3 | RESULTS

### 3.1 | Synthesis of p-SCN-Bn-TCMC-PSMA ligand (NG001)

The synthesis of the PSMA ligand p-SCN-Bn-TCMC-PSMA ligand (NG001) is summarized in Figure 1A. Compounds **1** and **2** (Figure 1A) were synthesized following procedures reported in literature.<sup>17,35</sup> In the final step, NG001 was synthesized by conjugating the isothiocyanato group of p-SCN-Bn-TCMC to the amino group of a PSMA binding intermediate. NG001 was characterized by  $^1\text{H}$  NMR, LC/MS and HPLC analyses (Figures S1-S3).

NG001 is different from PSMA-617 in several aspects (Figures 1B-1D and Table 1). Firstly, the DOTA chelator is replaced by a carbon substituted TCMC chelator that has all four chelator arms free (Figure 1B). Secondly, NG001 has an extended linker region including an isothiocyanatobenzyl linker. In contrast, PSMA-617 has a shorter linker region and uses one of the chelator arms as linker attachment (Figure 1C). Thus, the molecular weights, TPSAs, molecular volumes and solubility of the two molecules differ significantly (Table 1). Ten milligrams of PSMA-617 were completely dissolved in 1 mL of

**TABLE 1** Analytical data of NG001 and PSMA-617

Compound	Chemical Formula	MW, g/mol	Exact Mass <sup>e</sup>	<i>t<sub>r</sub></i> , min <sup>f</sup>	Chemical Purity <sup>g</sup>	LogP <sup>h</sup>	TPSA (Å <sup>2</sup> ) <sup>i</sup>	Volume (Å <sup>3</sup> ) <sup>j</sup>
NG001 <sup>a</sup>	C <sub>65</sub> H <sub>86</sub> F <sub>12</sub> N <sub>14</sub> O <sub>21</sub> S	1659.52 <sup>c</sup> 1203.43 <sup>d</sup>	1202.59	3.44	>98.0%	-4.63	420.60	1094.42
PSMA-617 <sup>b</sup>	C <sub>57</sub> H <sub>75</sub> F <sub>12</sub> N <sub>9</sub> O <sub>24</sub>	1498.25 <sup>c</sup> 1042.15 <sup>d</sup>	1041.50	3.15	>98.0%	-5.23	365.17	944.82

<sup>a</sup>(((1S)-1-carboxy-5-((2S)-3-(naphthalen-2-yl)-2-((1R,4S)-4-((3-(4-((1,4,7,10-tetrakis(2-amino-2-oxoethyl)-1,4,7,10-tetraazacyclododecan-2-yl)methyl)phenyl)thioureido)methyl)cyclohexane-1-carboxamido)propanamido)pentyl)carbamoyl)-L-glutamic acid; trifluoroacetic acid (1:4).

<sup>b</sup>(((S)-1-carboxy-5-((S)-3-(naphthalen-2-yl)-2-((1R,4S)-4-((2-(4,7,10-tris(carboxymethyl)-1,4,7,10-tetraazacyclododecan-1-yl)acetamido)methyl)cyclohexane-1-carboxamido)propanamido)pentyl)carbamoyl)-L-glutamic acid trifluoroacetic acid (1:4).

<sup>c</sup>Molecular weight with trifluoroacetic acid (1:4).

<sup>d</sup>Molecular weight without trifluoroacetic acid.

<sup>e</sup>Calculated using mass spectrometry data.

<sup>f</sup>Retention time of unlabelled ligands in a reversed phase HPLC (column Shim-pack XR-ODS). Mobile phase: A – water with 0.01% trifluoroacetic acid (TFA); B – acetonitrile with 0.01% TFA.

<sup>g</sup>Chemical purity was measured by HPLC.

<sup>h</sup>Logarithm of partition coefficient between n-octanol and water (LogP, Molinspiration calculations<sup>36</sup>).

<sup>i</sup>Topological polar surface area (TPSA Molinspiration calculations<sup>36</sup>).

<sup>j</sup>Molecular volume (Molinspiration calculations<sup>36</sup>).

0.5 M NH<sub>4</sub>OAc in 0.1 M HCl at pH 5 to 6 and temperatures 4 and 20°C. In contrast, NG001 precipitated at 4°C since it is more lipophilic than PSMA-617 and less soluble in aqueous buffer systems. NG001 becomes more soluble as temperature rises. The obtained results were supported by HPLC data (Figure 1D) and calculations (Table 1). NG001 had significantly higher retention on the reverse phase column than PSMA-617, which indicates a more hydrophobic (ie, more lipophilic) nature of NG001 (Figure 1D). The log *P* value of NG001 was determined to be -4.63 by Molinspiration software,<sup>36</sup> while the log *P* value of PSMA-617 was -5.23, indicating higher hydrophilic properties of PSMA-617 (Table 1).

### 3.2 | Radiolabelling and separation of [<sup>212</sup>Pb]Pb-NG001 from <sup>224</sup>Ra

Radiolabelling of PSMA-targeting ligands NG001 and PSMA-617 with <sup>212</sup>Pb was performed using a <sup>224</sup>Ra/<sup>212</sup>Pb-liquid generator solution, in which <sup>224</sup>Ra is in transient equilibrium with daughter nuclides. Radiolabelling of both ligands was efficient and fast with RCP above 90%. The TLC used for analysing labelling did not indicate any significant <sup>224</sup>Ra complexation with the ligands. This is in good agreement with previous data reported for the <sup>224</sup>Ra/<sup>212</sup>Pb-liquid generator, as described by Westrom et al.<sup>32</sup>

Lead-212-labelled NG001 was purified with a PD Minitrap G-10 column prepacked with Sephadex G-10 resin to remove <sup>224</sup>Ra and other unconjugated daughter radionuclides. The purification procedure had a high radiochemical yield of 85.9% in fractions 3 to 7, with fraction 4 accounting for almost 40% of the radioligand (Table 2). Fractions 3 to 5 had the highest radiochemical yield of 75.78±5.97% and RCP above 93%, and these fractions were used in further experiments.

The <sup>212</sup>Pb activity of the purified product (fractions 3-5) was measured after 4 to 5 days to determine the

**TABLE 2** Yield and radiochemical purity (RCP) ± SD of [<sup>212</sup>Pb]Pb-NG001 in the different fractions after purification with PD Minitrap G-10 columns prepacked with Sephadex G-10 resin, n=2-4

Fraction	Yield, %	RCP, %
3	15.12±10.53	96.83±0.69
4	38.68±3.64	96.08±0.43
5	21.98±8.89	93.25±1.24
6	6.96±1.82	89.97±6.55
7	3.15±0.76	89.36±6.41
Total	85.90±4.71	

amount of <sup>224</sup>Ra present in the sample. The data showed that 0.67±0.24% <sup>224</sup>Ra was present in the samples after purification (n=11).

### 3.3 | Radiolytic stability

Stability of [<sup>212</sup>Pb]Pb-NG001 stored in PBS or FBS in 1:1 ratio was tested by TLC analysis after 1, 4, 24 and 48 hours (Table 3). The radiolabelled ligand showed high stability when stored in both PBS and FBS, with RCP above 92% at all time points up to 48 hours.

### 3.4 | Binding and internalization of <sup>212</sup>Pb-labelled NG001 and PSMA-617 in C4-2 cells

Both radio ligands [<sup>212</sup>Pb]Pb-NG001 and [<sup>212</sup>Pb]Pb-PSMA-617 exhibited high affinity to C4-2 cells (Figure S4). They had similar *B*<sub>max</sub> values (approximately 370 000 antigens per cell) and *k*<sub>d</sub> values of 22.0±4.1 nM and 11.1±1.8 nM, respectively (Figure S4). Similar binding and internalization of both PSMA ligands were observed in C4-2 cells (Figure 2). [<sup>212</sup>Pb]Pb-NG001 showed binding ratios up to 31.9±3.0 %IA/10<sup>6</sup> cells and internalization ratios up to 21.0±7.94 %IA/10<sup>6</sup> cells, compared with 33.2±9.7% and 23.3±4.7%, respectively, for [<sup>212</sup>Pb]Pb-PSMA-617 (Figure 2).

### 3.5 | Biodistribution of [<sup>212</sup>Pb]Pb-NG001 and [<sup>212</sup>Pb]Pb-PSMA-617 in athymic mice bearing human prostate C4-2 xenografts

To study biodistribution, NG001 and PSMA-617 were radiolabelled with <sup>212</sup>Pb and separated from <sup>224</sup>Ra, as described above, and sterile-filtered immediately before intravenous injection in athymic mice bearing human prostate C4-2 cancer xenografts. Binding of the

**TABLE 3** Radiochemical purity (RCP) ± SD of purified [<sup>212</sup>Pb]Pb-NG001 diluted 1:1 in FBS or PBS after different time points up to 48 h, n=3

Incubation time, h	RCP, %	
	FBS	PBS
1	94.26±0.70	94.27±1.31
4	95.24±2.27	94.96±0.44
24	93.10±2.50	94.94±1.45
48	92.43±3.66	93.13±3.15

Abbreviations: FBS: fetal bovine serum; PBS: phosphate-buffered saline.



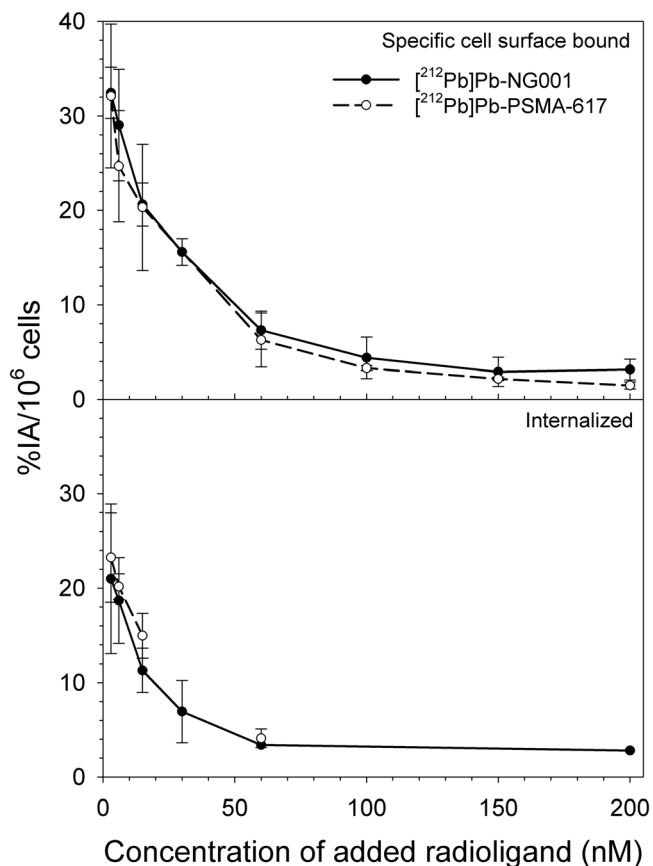


**FIGURE 2** Ratio of specific cell surface bound (top) and internalized (bottom) [<sup>212</sup>Pb]Pb-NG001 and [<sup>212</sup>Pb]Pb-PSMA-617 in C4-2 cells, expressed as percentage of added radioactivity (%IA) per 10<sup>6</sup> cells, n=2-5

radiolabelled ligands was verified by measuring cell binding ability in C4-2 cells. The cell binding fraction was around 45 to 50% for both radioligands.

The biodistribution data of [<sup>212</sup>Pb]Pb-NG001 and [<sup>212</sup>Pb]Pb-PSMA-617 are shown in Figures 3–5 and Tables S2 and S3. Both radioligands cleared rapidly from blood. At 2-hour post injection, there was only 0.48±0.10 %ID/g of [<sup>212</sup>Pb]Pb-NG001 in blood and three times lower activity (0.16±0.07 %ID/g) of [<sup>212</sup>Pb]Pb-PSMA-617 ( $P<.001$ ). Both radioligands were excreted mainly via the renal pathway yielding high initial levels in urine (Figure 3 and Table S2).

The uptake values (%ID/g) for tumour and kidneys at 2-hour post injection were 17.61±6.76 and 21.07±10.33 for [<sup>212</sup>Pb]Pb-NG001 and 17.93±2.90 and 52.82±26.62 for [<sup>212</sup>Pb]Pb-PSMA-617 (Figure 3 and Table S2). These data indicate considerably improved tumour to kidney ratio of NG001 compared with PSMA-617 (0.84 vs 0.34 after 2 hours,  $P<.05$ ; Figure 3 and Table S2), as well as rapid clearance of NG001 from kidneys. Hence, compared with [<sup>212</sup>Pb]Pb-PSMA-617, [<sup>212</sup>Pb]Pb-NG001 showed comparable tumour uptake ( $P>.05$ ) and 2.5-fold lower kidney uptake ( $P<.05$ ).

At 2-hour post injection, there was only 0.52±0.38 % ID/g of [<sup>212</sup>Pb]Pb-PSMA-617 in liver and 3 times higher activity (1.50±0.53 %ID/g) of [<sup>212</sup>Pb]Pb-NG001 ( $P<.05$ ). The uptake in salivary glands was low and similar (around 0.3 %ID/g) for both radioligands. The average uptake values for <sup>212</sup>Pb and <sup>212</sup>Bi were similar for both PSMA ligands (Figures 4 and 5), indicating no extensive

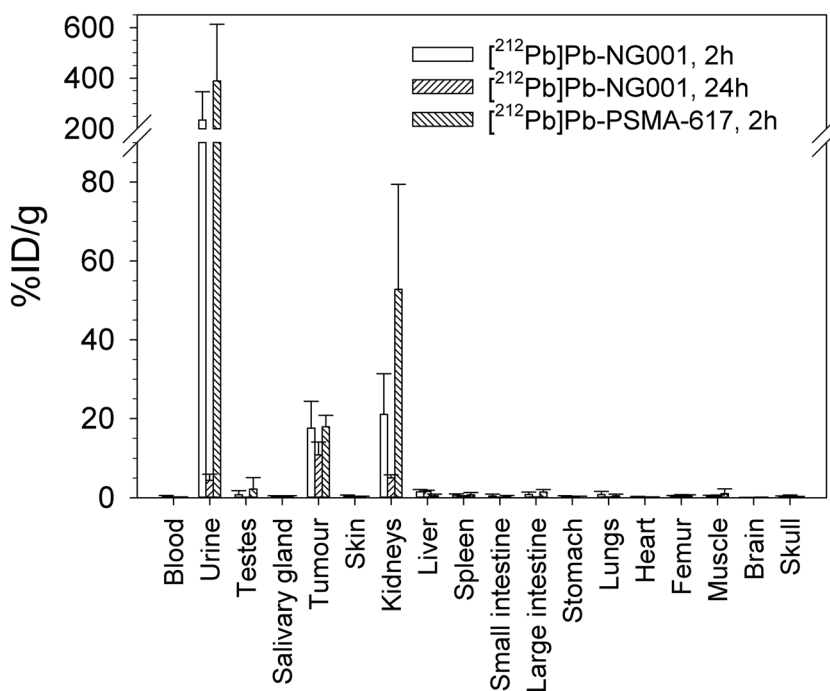


**FIGURE 3** Percentage of injected activity per gram of tissue (%ID/g) ± SD of [<sup>212</sup>Pb]Pb-NG001 and [<sup>212</sup>Pb]Pb-PSMA-617 at 2 and 24 hours after intravenous injection in athymic mice bearing human prostate C4-2 cancer xenografts, n=3-11 mice per group

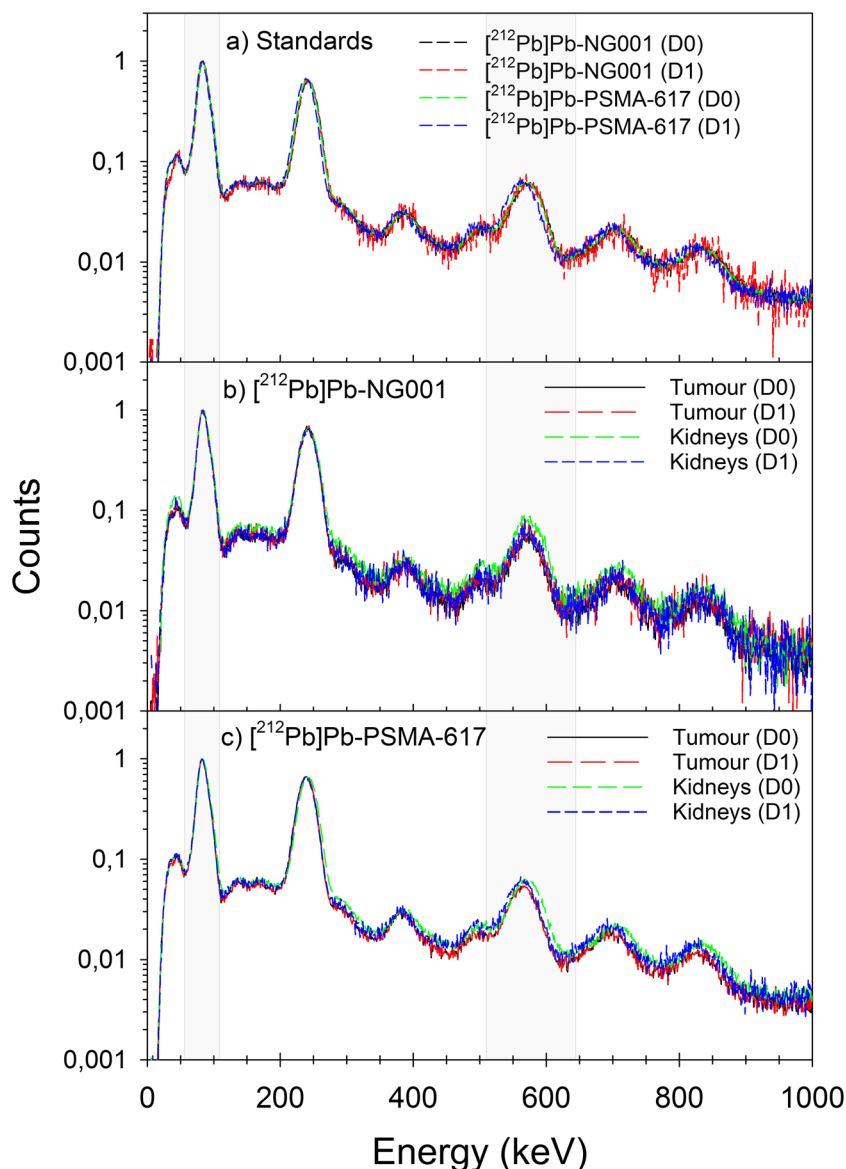


**FIGURE 4** Gamma-ray spectra obtained for the standards of  $[^{212}\text{Pb}]\text{Pb-NG001}$  and  $[^{212}\text{Pb}]\text{Pb-PSMA-617}$  (A) and of  $[^{212}\text{Pb}]\text{Pb-NG001}$  (B) and  $[^{212}\text{Pb}]\text{Pb-PSMA-617}$  (C) in tumour and in kidneys. Counts were normalized to 1 at 83 keV. Mice were sacrificed 2 hour post injection. Counts of organs and standards were performed within 1 hour after sacrifice (Day 0) and the next day (D1, at equilibrium). The counts in the 60 to 110 keV window were assumed to count mainly X-rays and gamma radiation from  $^{212}\text{Pb}$ . The 520 to 640 keV window was used to determine  $^{212}\text{Bi}$  indirectly from the highly abundant  $^{208}\text{Tl}$  gamma radiation. To quantify the amount of  $^{212}\text{Bi}$  correctly, samples were measured after approximately 30-60 minutes, when transient equilibrium between  $^{208}\text{Tl}$  and the  $^{212}\text{Bi}$  parent had been established

translocalization of  $^{212}\text{Bi}$  from  $^{212}\text{Pb}$  in the studied organs.

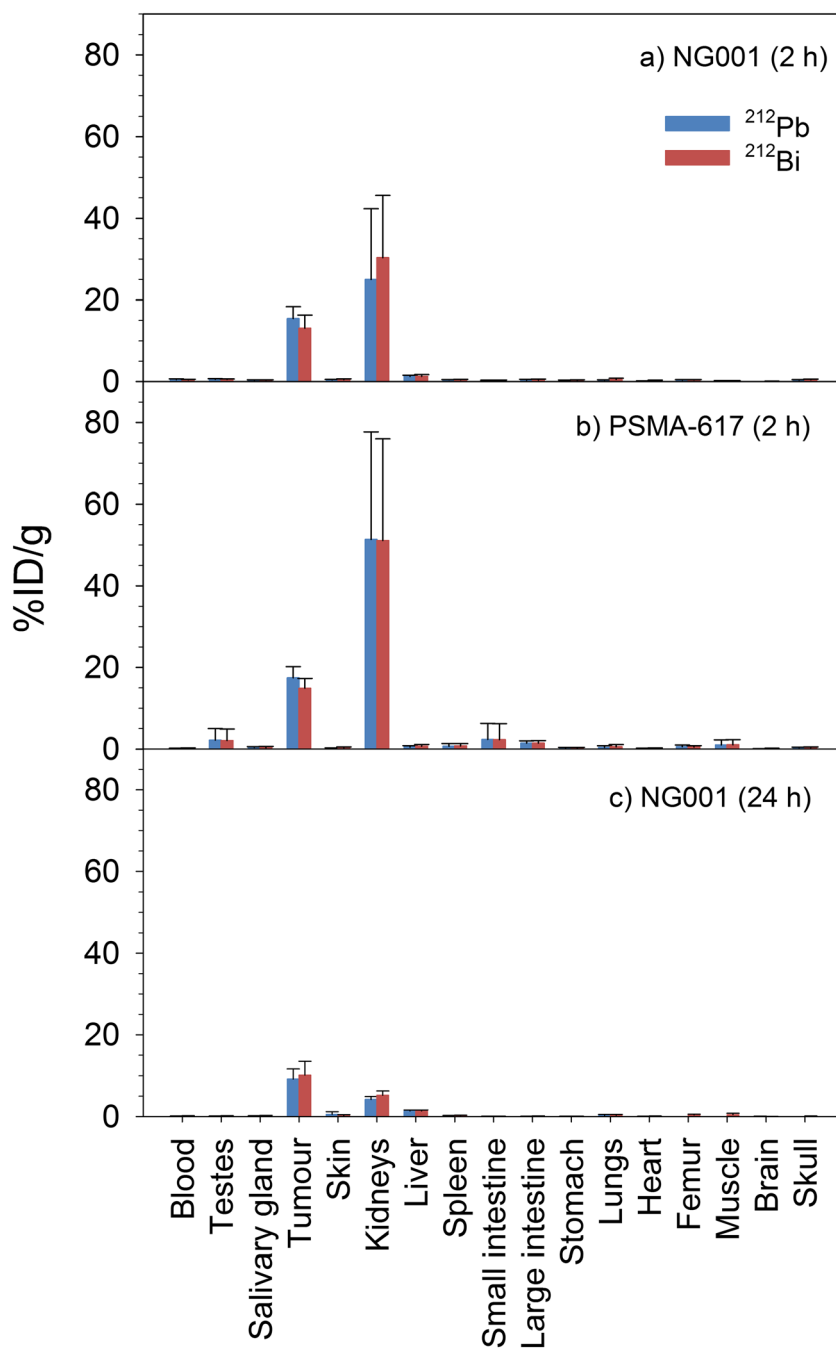
## 4 | DISCUSSION

The present study aimed to label NG001 and PSMA-617 with  $^{212}\text{Pb}$  and to compare their in vitro and in vivo behaviour. NG001 consists of a highly specific urea-based PSMA-binding motif and the TCMC chelator. The linker and binding motif in PSMA inhibitors both influence affinity and internalization, while chelator and linker have high impact on the pharmacokinetic profile regarding tumour and kidney uptake.<sup>8,30,31,39</sup> Also, the conjugation linker for the chelator is of importance. One improvement of NG001 is that the chelator unit has all four arms free due to the use of a backbone substituted

linker instead of using one of the chelator arms for the linking purpose, as in PSMA-617.

Radiolabelling of PSMA-targeting ligands with  $^{212}\text{Pb}$  was carried out by the recently introduced method using the  $^{224}\text{Ra}/^{212}\text{Pb}$ -liquid generator.<sup>32</sup> NG001 was labelled with  $^{212}\text{Pb}$  at pH 4 to 8 and without the need for heating the reaction solution. Using Sephadex G-10 size exclusion gel filtration,  $[^{212}\text{Pb}]\text{Pb-NG001}$  was purified with 85% yield (Table 2) and with less than 1% breakthrough of  $^{224}\text{Ra}$ . PSMA-617 was also efficiently labelled with  $^{212}\text{Pb}$  and purified to remove free  $^{224}\text{Ra}$  and other unconjugated daughter nuclides (data not shown). Thus, a product with relevant quantity and purity can be prepared by a simple procedure using the  $^{224}\text{Ra}/^{212}\text{Pb}$ -liquid generator system for  $^{212}\text{Pb}$ . In several preclinical and clinical studies,  $^{212}\text{Pb}$  has been eluted with concentrated HCl from the  $^{224}\text{Ra}/^{212}\text{Pb}$ -generator.<sup>18,24,30</sup> In contrast, the method used

**FIGURE 5** Percentage of injected activity per gram of tissue (%ID/g)  $\pm$  SD of  $^{212}\text{Pb}$ - and  $^{212}\text{Bi}$ -labelled NG001 (A) and PSMA-617 (B) at 2 hour and NG001 at 24 hour (C) post injection in athymic mice bearing human prostate C4-2 cancer xenografts,  $n=3-4$  mice. The values for  $^{212}\text{Pb}$  are corrected for  $^{212}\text{Pb}$  decay and  $^{212}\text{Pb}$  ingrowth from  $^{224}\text{Ra}$



in the present study is more advantageous since the steps involving handling and evaporation of concentrated acid solutions with high radioactivity levels can be avoided. In a given setting, this reduces the on-site preparation time that only involves radiolabelling (~30 minutes) and removal of  $^{224}\text{Ra}$  performed by simple desalting gel exclusion separation (~15 minutes). Radium-224 is not suitable for conjugation to targeting molecules,<sup>40,41</sup> and it is neither chelated by DOTA nor TCMC.

A good stability of [ $^{212}\text{Pb}$ ]Pb-NG001 within 48 hours in PBS and serum was demonstrated by TLC analyses (Table 3). However, the affinity of the PSMA ligand for

its binding site may decrease with time.<sup>42,43</sup> PSMA ligand integrity is difficult to maintain in formulations consisting of alpha- or beta-emitting radionuclides due to direct radiation damage (autoradiolysis) and indirect radiation damage (radical-induced radiolysis). Radiolysed radioligands have reduced receptor affinity,<sup>42,43</sup> and, therefore, will lead to decreased therapeutic and diagnostic efficacy, and circulation in the body with increased radiation toxicity to organs such as liver and bone marrow. Radiolysis induced by free radicals can be prevented by radioprotectants, such as ascorbic acid, human serum albumin, cysteamine and glycerol.<sup>42,43</sup>

An *in vitro* binding study of [ $^{212}\text{Pb}$ ]Pb-NG001 and [ $^{212}\text{Pb}$ ]Pb-PSMA-617 to C4-2 cells yielded  $k_d$  values of 22.0 and 11.1 nM, respectively (Figure S4), which are in agreement with other studies that have examined the binding of PSMA ligands to PSMA-positive cells.<sup>44-46</sup> Gourni et al showed that [ $^{111}\text{In}$ ]In-PSMA-617 to LNCaP cells yielded a  $k_d$  of 5.4 nM.<sup>44</sup> Umbricht et al reported that [ $^{177}\text{Lu}$ ]Lu-PSMA-617, [ $^{44}\text{Sc}$ ]Sc-PSMA-617 and [ $^{68}\text{Ga}$ ]Ga-PSMA-617 to PC-3 PIP cells gave the  $k_d$  values of 39, 33 and 72 nM, respectively.<sup>45</sup>

Comparable *in vitro* and *in vivo* behaviour of [ $^{203}\text{Pb}$ ]Pb-CA009 and [ $^{212}\text{Pb}$ ]Pb-NG001 was expected due to the chemical similarities of  $^{203}\text{Pb}$  and  $^{212}\text{Pb}$  with regard to their labelling with CA009/NG001. The cell surface binding and internalization rates were 106.5 %IA and 27.4 %IA per  $10^6$  C4-2 cells, respectively, for [ $^{203}\text{Pb}$ ]Pb-CA009<sup>31</sup> after 45-minute incubation,<sup>31</sup> whereas the cell surface bound fraction was 7 times lower (15.6 %IA per  $10^6$  C4-2 cells) and internalized fraction was 4 times lower (6.9 %IA per  $10^6$  C4-2 cells) for [ $^{212}\text{Pb}$ ]Pb-NG001 after the same time of incubation (Figure 2). In both cases, 30 nM solutions of Pb-labelled compounds were compared. There are several possible explanations for such discrepancies: differences in protocols and analysis for the determination of cell surface binding and internalization rates, C4-2 cells were grown at different conditions, different specific activities of radioligands, the variations in the extracellular and intracellular stability of the radioligands.

The tumour uptake of [ $^{212}\text{Pb}$ ]Pb-NG001 (Figure 3 and Table S3) was compared with that of the most promising PSMA ligands CA012 and L2.<sup>30,31</sup> For *in vivo* studies, Dos Santos et al have chosen another PSMA ligand CA012 due to faster kidney clearance than CA009.<sup>31</sup> In C4-2 tumour-bearing BALB/c nu/nu mice, [ $^{203}\text{Pb}$ ]Pb-CA012 showed a tumour uptake of 8.4 %ID/g at 1-hour and of 3.3 %ID/g at 24-hours after injection,<sup>31</sup> which was considerably lower than the tumour uptake of 17.6 %ID/g at 2-hour and of 10.9 %ID/g at 24-hour for [ $^{212}\text{Pb}$ ]Pb-NG001 in C4-2 tumour-bearing Hsd: Athymic Nude-Foxn1<sup>nu</sup> mice (Figure 3). In a study conducted by Banerjee et al, the tumour accumulation was 25.2 %ID/g at 2-hour and 8.5 %ID/g at 24-hour for the ligand chosen for the therapeutic studies, [ $^{203}\text{Pb}$ ]Pb-TCMC-L2, in NOD-SCID mice bearing PC3-PIP tumours.<sup>30</sup> The obtained values for [ $^{212}\text{Pb}$ ]Pb-NG001 (at 2-hour) are higher than that reported for [ $^{203}\text{Pb}$ ]Pb-CA012 (at 1-hour) for the same tumours<sup>31</sup> and 1.5 times lower than that of [ $^{203}\text{Pb}$ ]Pb-L2 (at 2-hour), where PC3-PIP tumours were studied.<sup>30</sup> However, much faster clearance of [ $^{203}\text{Pb}$ ]Pb-CA012 and [ $^{203}\text{Pb}$ ]Pb-L2 than of [ $^{212}\text{Pb}$ ]Pb-NG001 in tumours was observed after 24 hours. Tumours lost 61% and 66% of the initial activity (at 1-2 hours) of [ $^{203}\text{Pb}$ ]Pb-CA012 and [ $^{203}\text{Pb}$ ]Pb-L2, respectively,<sup>30,31</sup> and only 27%

the initial activity (2 hours) of [ $^{212}\text{Pb}$ ]Pb-NG001 (Figure 3).

Although [ $^{212}\text{Pb}$ ]Pb-NG001 and [ $^{212}\text{Pb}$ ]Pb-PSMA-617 displayed similar *in vitro* characteristics regarding affinity, internalization (Figure 2) and *in vivo* tumour uptake (Figure 3), the kidney uptake was 2.5-fold lower for [ $^{212}\text{Pb}$ ]Pb-NG001 compared with [ $^{212}\text{Pb}$ ]Pb-PSMA-617 at the 2-hour time point. This is compatible with findings by Banerjee et al<sup>30</sup> showing that TCMC-chelated ligands displayed approximately twofold reduced renal uptake compared with DOTA and DOTA-mono amide chelating agents. The reduced kidney uptake of NG001 is important for the use of  $^{212}\text{Pb}$  in RLT against PSMA-expressing prostate cancer.

Due to the high hydrophilicity of both compounds, they are eliminated by the kidneys and almost no unspecific uptake in nontarget tissue was observed (Figure 3). Lower kidney uptake, somewhat higher liver uptake, longer retention in blood circulation and in tumour of [ $^{212}\text{Pb}$ ]Pb-NG001 in comparison to [ $^{212}\text{Pb}$ ]Pb-PSMA-617 (Figure 3 and Table S2) seem to be related to the lower hydrophilicity of NG001. The direct comparison of PSMA ligand data from various groups is not easy since different mouse strains, cell lines and different specific activities of radioligands were used in the various studies. PC3-PIP cells have higher PSMA expression than C4-2 cells.<sup>47-49</sup> However, our results clearly indicate that efficient targeting of PSMA-tumours can be achieved with [ $^{212}\text{Pb}$ ]Pb-NG001, which is rapidly cleared from the body but not from the tumour (Figure 3).

Previous studies have demonstrated that there is PSMA expression in normal kidney proximal tubular epithelial cells.<sup>50</sup> Hence, radiation toxicity to kidneys due to the fast clearance of radioligands through the urinary tract is of concern for their application for RLT.<sup>6,51</sup> However, neither acute nor long-term kidney toxicity has recently been reported to be a clinical problem in patients treated with [ $^{177}\text{Lu}$ ]Lu-PSMA-617.<sup>51</sup> It is noteworthy that human kidneys have lower PSMA expression than mouse kidneys.<sup>52</sup> Therefore, the human kidney dose cannot be directly extrapolated from mouse kidney uptake with PSMA-binding ligands. A direct comparison of [ $^{177}\text{Lu}$ ]Lu-PSMA-617 and [ $^{177}\text{Lu}$ ]Lu-PSMA-I&T in mice demonstrated that [ $^{177}\text{Lu}$ ]Lu-PSMA-617 had higher tumour uptake and lower kidney and salivary gland uptake compared with [ $^{177}\text{Lu}$ ]Lu-PSMA-I&T.<sup>8</sup> An almost tenfold faster clearance in mice was observed with [ $^{177}\text{Lu}$ ]Lu-PSMA-617.<sup>8</sup> In contrast, a direct comparison of both radioligands in patients demonstrated similar uptake in kidneys and tumours and higher uptakes of [ $^{177}\text{Lu}$ ]Lu-PSMA-617 in salivary glands.<sup>9</sup>

It has been reported that about one third of  $^{212}\text{Bi}$  atoms dissociate from the chelator when  $^{212}\text{Pb}$  decays.<sup>32</sup> As [ $^{212}\text{Pb}$ ]Pb-NG001 is internalized after binding to PSMA on C4-2 cells (Figure 2), its internalization could contribute to increased TAT efficacy and decreased systemic toxicity. Internalization may help retaining radioisotope daughters (including the two alpha emitters  $^{212}\text{Bi}$  and  $^{212}\text{Po}$ , and the beta emitter  $^{208}\text{Tl}$ ) within the cytoplasm of targeted cells, since diffusion of metal ions across the cell membrane would be very slow. Loss of  $^{212}\text{Bi}$  from circulating [ $^{212}\text{Pb}$ ]Pb-NG001 could allow  $^{212}\text{Bi}$  to redistribute and irradiate normal tissues. However, in the present study, no differences were detected between the biodistribution of  $^{212}\text{Pb}$  and  $^{212}\text{Bi}$  in different organs (Figures 4 and 5), indicating that translocalization of  $^{212}\text{Bi}$  seems not to be a significant problem with [ $^{212}\text{Pb}$ ]Pb-NG001. The rapid clearance of [ $^{212}\text{Pb}$ ]Pb-NG001 in mice likely prevented measurable amounts of  $^{212}\text{Bi}$  from being released.

The presence of  $^{224}\text{Ra}$  as a contaminant in the  $^{212}\text{Pb}$  products could potentially present an unwanted hazard but as long as it is kept at less than 1%, it will probably not be a significant problem in terms of product safety. The majority of patients (up to 90%) with late stage mCRPC have bone metastases.<sup>53</sup> The alpha-emitting  $^{223}\text{Ra}$  is a natural bone-seeker, and it is approved for the treatment of mCRPC patients with bone metastases, but it is not suitable for patients with documented extraskelatal disease.<sup>54</sup> Radium-224 also targets stromal elements in osteoblastic metastatic lesions.<sup>55,56</sup> Patients treated with 100 MBq of [ $^{212}\text{Pb}$ ]Pb-NG001 should not get more than 1 MBq of  $^{224}\text{Ra}$ . Radium-224 was used earlier for many years for the treatment of different noncancerous diseases, and the risk assessment demonstrated that 1 MBq of  $^{224}\text{Ra}$  per dosing, or a total of 10 MBq cumulative, is acceptable for adult patients.<sup>55</sup>

## 5 | CONCLUSION

The PSMA ligand, NG001, was synthesized by conjugating the isothiocyanato group of p-SCN-Bn-TCMC to the amino group of a glutamate-urea-based PSMA binding entity. NG001 is different from PSMA-617 in that the DOTA chelator is replaced by the TCMC chelator, NG001 has an extended linker region and is less hydrophilic than PSMA-617. Both ligands were efficiently labelled with  $^{212}\text{Pb}$  using a  $^{224}\text{Ra}/^{212}\text{Pb}$ -solution generator in transient equilibrium with progeny. Lead-212-labelled NG001 was purified with a radiochemical yield of 86% and with less than 1% breakthrough of  $^{224}\text{Ra}$ . A good stability of [ $^{212}\text{Pb}$ ]Pb-NG001 up to 48 hours in

serum was demonstrated. Compared with [ $^{212}\text{Pb}$ ]Pb-PSMA-617, [ $^{212}\text{Pb}$ ]Pb-NG001 displayed a similar binding and internalization in PSMA-positive C4-2 cells, and comparable tumour uptake but almost a 2.5-fold lower kidney uptake in mice bearing C4-2 tumours. No difference was detected between the biodistribution of  $^{212}\text{Pb}$  and  $^{212}\text{Bi}$  during the 24-hour study period, indicating that translocalization of  $^{212}\text{Bi}$  was low. The rapid clearance and targeting, as well as internalization of [ $^{212}\text{Pb}$ ]Pb-NG001, likely prevented measurable amounts of  $^{212}\text{Bi}$  from being released. In conclusion, the obtained results warrant further preclinical studies to evaluate the therapeutic efficacy of [ $^{212}\text{Pb}$ ]Pb-NG001.

## ACKNOWLEDGEMENTS

The study was financially supported by Sciencons AS (Oslo, Norway), Nucligen AS (Oslo, Norway) and the Norwegian Research Council (Oslo, Norway).

## DISCLOSURE STATEMENT

R. H. L holds ownership interest in Sciencons AS. R. H. L., A. J., Ø. S. B. and V. Y. S. hold ownership interest in Nucligen AS.

## ORCID

Vilde Yuli Stenberg  <https://orcid.org/0000-0003-4329-5411>

Asta Juzeniene  <https://orcid.org/0000-0001-9426-0062>

Qingqi Chen  <https://orcid.org/0000-0002-1892-5365>

Xiaoming Yang  <https://orcid.org/0000-0002-7099-9863>

Øyvind Sverre Bruland  <https://orcid.org/0000-0003-1631-3733>

## REFERENCES

- Hupei MC, Philippi C, Roth D, et al. Expression of prostate-specific membrane antigen (PSMA) on biopsies is an independent risk stratifier of prostate cancer patients at time of initial diagnosis. *Front Oncol.* 2018;8:623–629.
- Paschalis A, Sheehan B, Riisnaes R, et al. Prostate-specific membrane antigen heterogeneity and DNA repair defects in prostate cancer. *Eur Urol.* 2019;76(4):469–478.
- Chakravarty R, Siamof CM, Dash A, Cai W. Targeted alpha-therapy of prostate cancer using radiolabeled PSMA inhibitors: a game changer in nuclear medicine. *Am J Nucl Med Mol Imaging.* 2018;8(4):247–267.
- Cimadamore A, Cheng M, Santoni M, et al. New prostate cancer targets for diagnosis, imaging, and therapy: focus on prostate-specific membrane antigen. *Front Oncol.* 2018;8:653–663.
- Lutje S, Slavik R, Fendler W, Herrmann K, Eiber M. PSMA ligands in prostate cancer—probe optimization and theranostic applications. *Methods.* 2017;130:42–50.
- Kuo HT, Pan J, Zhang Z, et al. Effects of linker modification on tumor-to-kidney contrast of ( $^{68}\text{Ga}$ )-Labeled PSMA-targeted imaging probes. *Mol Pharm.* 2018;15(8):3502–3511.

7. Benesova M, Schafer M, Bauder-Wust U, et al. Preclinical evaluation of a Tailor-made DOTA-conjugated PSMA inhibitor with optimized linker moiety for imaging and endoradiotherapy of prostate cancer. *J Nucl Med*. 2015;56(6):914-920.
8. Banerjee SR, Kumar V, Lisok A, et al. (177)Lu-labeled low-molecular-weight agents for PSMA-targeted radiopharmaceutical therapy. *Eur J Nucl Med Mol Imaging*. 2019;46(12):2545-2557.
9. Kulkarni HR, Singh A, Schuchardt C, et al. PSMA-based radioligand therapy for metastatic castration-resistant prostate cancer: the Bad Berka Experience Since 2013. *J Nucl Med*. 2016;57(Suppl 3):97s-104s.
10. Yadav MP, Ballal S, Sahoo RK, Dwivedi SN, Bal C. Radioligand Therapy With (177)Lu-PSMA for metastatic castration-resistant prostate cancer: a systematic review and meta-analysis. *AJR Am J Roentgenol*. 2019;213(2):275-285.
11. Afshar-Oromieh A, Haberkorn U, Zechmann C, et al. Repeated PSMA-targeting radioligand therapy of metastatic prostate cancer with (131)I-MIP-1095. *Eur J Nucl Med Mol Imaging*. 2017;44(6):950-959.
12. Kratochwil C, Bruchertseifer F, Giesel FL, et al. 225Ac-PSMA-617 for PSMA-targeted alpha-radiation therapy of metastatic castration-resistant prostate cancer. *J Nucl Med*. 2016;57(12):1941-1944.
13. Kratochwil C, Bruchertseifer F, Rathke H, et al. Targeted alpha-therapy of metastatic castration-resistant prostate cancer with (225)Ac-PSMA-617: Swimmer-plot analysis suggests efficacy regarding duration of tumor control. *J Nucl Med*. 2018;59(5):795-802.
14. Satheke M, Knoesen O, Meckel M, Modiselle M, Vorster M, Marx S. (213)Bi-PSMA-617 targeted alpha-radionuclide therapy in metastatic castration-resistant prostate cancer. *Eur J Nucl Med Mol Imaging*. 2017;44(6):1099-1100.
15. Robertson AKH, Ramogida CF, Schaffer P, Radchenko V. Development of (225)Ac radiopharmaceuticals: TRIUMF perspectives and experiences. *Curr Radiopharm*. 2018;11(3):156-172.
16. Morgenstern A, Apostolidis C, Kratochwil C, Satheke M, Krolicki L, Bruchertseifer F. An overview of targeted alpha therapy with (225)actinium and (213)bismuth. *Curr Radiopharm*. 2018;11(3):200-208.
17. Chappell LL, Dadachova E, Milenic DE, Garmestani K, Wu C, Brechbiel MW. Synthesis, characterization, and evaluation of a novel bifunctional chelating agent for the lead isotopes 203Pb and 212Pb. *Nucl Med Biol*. 2000;27(1):93-100.
18. Baidoo KE, Milenic DE, Brechbiel MW. Methodology for labeling proteins and peptides with lead-212 (212Pb). *Nucl Med Biol*. 2013;40(5):592-599.
19. Yong K, Brechbiel M. Application of (212)Pb for Targeted alpha-particle therapy (TAT): pre-clinical and mechanistic understanding through to clinical translation. *AIMS Med Sci*. 2015;2(3):228-245.
20. Mirzadeh S, Kumar K, Gansow OA. The chemical fate of <sup>212</sup>Bi-DOTA formed by b-decay of <sup>212</sup>Pb(DOTA)<sup>2-\*,\*\*</sup>. *Radiochimica Acta*. 1993;60:1-10.
21. Yong K, Brechbiel MW. Towards translation of 212Pb as a clinical therapeutic; getting the lead in! *Dalton Trans*. 2011;40(23):6068-6076.
22. Horak E, Hartmann F, Garmestani K, et al. Radioimmunotherapy targeting of HER2/neu oncoprotein on ovarian tumor using lead-212-DOTA-AE1. *J Nucl Med*. 1997;38(12):1944-1950.
23. Ruble G, Wu C, Squire RA, Gansow OA, Strand M. The use of 212Pb-labeled monoclonal antibody in the treatment of murine erythroleukemia. *Int J Radiat Oncol Biol Phys*. 1996;34(3):609-616.
24. Meredith RF, Torgue JJ, Rozgaja TA, et al. Safety and outcome measures of first-in-human intraperitoneal alpha radioimmunotherapy with 212Pb-TCMC-trastuzumab. *Am J Clin Oncol*. 2018;41(7):716-721.
25. Delpassand E, Tworowska I, Shanon F, et al. First clinical experience using targeted alpha-emitter therapy with 212Pb-DOTAMTATE (AlphaMedix TM) in patients with SSTR(+) neuroendocrine tumors. *J Nucl Med*. 2019;60:559.
26. Yordanova A, Becker A, Eppard E, et al. The impact of repeated cycles of radioligand therapy using [(177)Lu]Lu-PSMA-617 on renal function in patients with hormone refractory metastatic prostate cancer. *Eur J Nucl Med Mol Imaging*. 2017;44(9):1473-1479.
27. Baum RP, Kulkarni HR, Schuchardt C, et al. 177Lu-Labeled prostate-specific membrane antigen radioligand therapy of metastatic castration-resistant prostate cancer: safety and efficacy. *J Nucl Med*. 2016;57(7):1006-1013.
28. Kelly JM, Amor-Coarasa A, Ponnala S, et al. A single dose of (225)Ac-RPS-074 induces a complete tumor response in an LNCaP Xenograft Model. *J Nucl Med*. 2019;60(5):649-655.
29. Kiess AP, Minn I, Vaidyanathan G, et al. (2S)-2-(3-(1-Carboxy-5-(4-211At-Astatobenzamido)Pentyl)Ureido)-pentanedioic acid for PSMA-targeted alpha-particle radiopharmaceutical therapy. *J Nucl Med*. 2016;57(10):1569-1575.
30. Banerjee SR, Minn IL, Kumar V, et al. Preclinical evaluation of 203/212Pb-labeled low-molecular-weight compounds for targeted radiopharmaceutical therapy of prostate cancer. *J Nucl Med*. 2020;61:80-88.
31. Dos Santos JC, Schafer M, Bauder-Wust U, et al. Development and dosimetry of (203)Pb/(212)Pb-labelled PSMA ligands: bringing "the lead" into PSMA-targeted alpha therapy? *Eur J Nucl Med Mol Imaging*. 2019;46(5):1081-1091.
32. Westrom S, Generalov R, Bonsdorff TB, Larsen RH. Preparation of (212)Pb-labeled monoclonal antibody using a novel (224)Ra-based generator solution. *Nucl Med Biol*. 2017;51:1-9.
33. Hassfjell SP, Bruland OS, Hoff P. 212Bi-DOTMP: an alpha particle emitting bone-seeking agent for targeted radiotherapy. *Nucl Med Biol*. 1997;24(3):231-237.
34. Larsen RH. Lead and Thorium compounds. US patent number: US10377778B2. 2019.
35. Eder M, Kopka K, Schäfer M, Bauder-Wust U, Haberkorn U, Eisenhut M, Mier W, and Benesova M, Labeled inhibitors of prostate specific membrane antigen (psma), their use as imaging agents and pharmaceutical agents for the treatment of prostate cancer. 2013: USA.
36. Molinspiration Cheminformatics, <https://www.molinspiration.com/>. 2019 [cited 03.12.2019].
37. Ertl P, Rohde B, Selzer P. Fast calculation of molecular polar surface area as a sum of fragment-based contributions and its

- application to the prediction of drug transport properties. *J Med Chem.* 2000;43(20):3714-3717.
38. Larsen RH, Radiopharmaceutical solutions with advantageous properties. US patent number: US9433690B1.2016.
39. Wustemann T, Bauder-Wust U, Schafer M, et al. Design of internalizing PSMA-specific Glu-ureido-based radiotherapeutics. *Theranostics.* 2016;6(8):1085-1095.
40. Henriksen G, Hoff P, Larsen RH. Evaluation of potential chelating agents for radium. *Appl Radiat Isot.* 2002;56(5):667-671.
41. Gott M, Yang P, Kortz U, Stephan H, Pietzsch HJ, Mamat C. A (224)Ra-labeled polyoxopalladate as a putative radiopharmaceutical. *Chem Commun (Camb).* 2019;55(53):7631-7634.
42. Umbricht CA, Benesova M, Schibli R, Muller C. Preclinical development of novel PSMA-targeting radioligands: Modulation of albumin-binding properties to improve prostate cancer therapy. *Mol Pharm.* 2018;15(6):2297-2306.
43. Stallons TAR, Saidi A, Tworowska I, Delpassand ES, Torgue JJ. Preclinical investigation of (212)Pb-DOTAMTATE for peptide receptor radionuclide therapy in a neuroendocrine tumor model. *Mol Cancer Ther.* 2019;18(5):1012-1021.
44. Gourni E, Canovas C, Goncalves V, Denat F, Meyer PT, Maecke HR. (R)-NODAGA-PSMA: A versatile precursor for radiometal labeling and nuclear imaging of PSMA-positive tumors. *PLoS One.* 2015;10(12):1-16, e0145755.
45. Umbricht CA, Benesova M, Schmid RM, et al. (44)Sc-PSMA-617 for radiotheragnostics in tandem with (177)Lu-PSMA-617: preclinical investigations in comparison with (68)Ga-PSMA-11 and (68)Ga-PSMA-617. *EJNMMI Res.* 2017;7(1):9-18.
46. Eppard E, de la Fuente A, Benesova M, et al. Clinical translation and first in-human use of [(44)Sc]Sc-PSMA-617 for PET imaging of metastasized castrate-resistant prostate cancer. *Theranostics.* 2017;7(18):4359-4369.
47. Fan X, Wang L, Guo Y, et al. Ultrasonic Nanobubbles Carrying Anti-PSMA Nanobody: Construction and application in prostate cancer-targeted imaging. *PLoS One.* 2015;10(6):1-13, e0127419.
48. Castanares MA, Copeland BT, Chowdhury WH, et al. Characterization of a novel metastatic prostate cancer cell line of LNCaP origin. *Prostate.* 2016;76(2):215-225.
49. Michalska M, Schultze-Seemann S, Bogatyreva L, Hauschke D, Wetterauer U, Wolf P. In vitro and in vivo effects of a recombinant anti-PSMA immunotoxin in combination with docetaxel against prostate cancer. *Oncotarget.* 2016;7(16):22531-22542.
50. Mhaweche-Fauceglia P, Zhang S, Terracciano L, et al. Prostate-specific membrane antigen (PSMA) protein expression in normal and neoplastic tissues and its sensitivity and specificity in prostate adenocarcinoma: an immunohistochemical study using multiple tumour tissue microarray technique. *Histopathology.* 2007;50(4):472-483.
51. Gallyamov M, Meyrick D, Barley J, Lenzo N. Renal outcomes of radioligand therapy: experience of 177lutetium—prostate-specific membrane antigen ligand therapy in metastatic castrate-resistant prostate cancer. *Clin Kidney J.* 2019;1-7.sfz101. <https://doi.org/10.1093/ckj/sfz1101>
52. Bacich DJ, Pinto JT, Tong WP, Heston WD. Cloning, expression, genomic localization, and enzymatic activities of the mouse homolog of prostate-specific membrane antigen/NAALADase/folate hydrolase. *Mamm Genome.* 2001;12(2):117-123.
53. Tannock IF, de Wit R, Berry WR, et al. Docetaxel plus prednisone or mitoxantrone plus prednisone for advanced prostate cancer. *N Engl J Med.* 2004;351(15):1502-1512.
54. Parker C, Finkelstein SE, Michalski JM, et al. Efficacy and safety of radium-223 dichloride in symptomatic castration-resistant prostate cancer patients with or without baseline opioid use from the phase 3 ALSYMPCA trial. *Eur Urol.* 2016;70(5):875-883.
55. Lassmann M, Nosske D, Reiners C. Therapy of ankylosing spondylitis with 224Ra-radium chloride: dosimetry and risk considerations. *Radiat Environ Biophys.* 2002;41(3):173-178.
56. Juzeniene A, Bernoulli J, Suominen M, Halleen J, Larsen RH. Antitumor activity of novel bone-seeking, alpha-emitting (224)Ra-solution in a breast cancer skeletal metastases model. *Anti-cancer Res.* 2018;38(4):1947-1955.

## SUPPORTING INFORMATION

Additional supporting information may be found online in the Supporting Information section at the end of this article.

**How to cite this article:** Stenberg VY, Juzeniene A, Chen Q, Yang X, Bruland ØS, Larsen RH. Preparation of the alpha-emitting prostate-specific membrane antigen targeted radioligand [<sup>212</sup>Pb]Pb-NG001 for prostate cancer. *J Label Compd Radiopharm.* 2020;63:129–143. <https://doi.org/10.1002/jlcr.3825>